**TITLE** (maximum 150 characters)

# Predictive Ophthalmic Simulation Using Personalized Eye Models

**Authors:**

Ying-Ling A. Chen, Jim W.L. Lewis, Lei Shi, Ming Wang, Kevin Baker, Lance Kugler, and Bo Tan

**Authors: institution(s)/affiliation(s) for each author:**

Ying-Ling A. Chen

411 B. H. Goethert Parkway Tullahoma TN 37388

Center for Laser Applications

University of Tennessee Space Institute

ychen@utsi.edu

Jim W.L. Lewis

University of Tennessee Space Institute

jwllut@yahoo.com

Lei Shi

Center for Laser Applications

University of Tennessee Space Institute

lshi@utsi.edu

Ming Wang

Wang Vision Institute, Nashville

University of Tennessee Health Science Center, Memphis

drwang@wangvisioninstitute.com

Kevin Baker

University of Tennessee Space Institute

kbaker@utsi.edu

Bo Tan

School of Optometry

University of California at Berkeley

btan04@gmail.com

**Corresponding author:** Ying-Ling A. Chen

**Keywords:** computation, simulation, ophthalmic, personalized, schematic, optical, eye, model, keratoconus, instrumentation

**Short Abstract:** Computational optical models of human eyes that incorporate clinical measurements of healthy and diseased eyes can be constructed with contemporary optical design programs. The eye model bank and computations can provide sufficiently accurate ophthalmic measurement simulations to offer aspects of virtual clinical trial, a revolutionary approach for developing new instruments.

**Long Abstract:** (150 words minimum, 400 words maximum)

Throughout the 20th century, schematic eye models of increasing complexity were developed to represent and describe the average anatomical and optical properties of healthy adult eyes[1-5]. These models were valuable to evaluate optical performance, to investigate ocular properties, and to design new ophthalmic corrections [6]. However, an individual's eye can be very different from any of these models.

More recently, the demand for improved vision quality has made available high precision digital ophthalmic data for individuals. Ultrasound A- and B-scans, MRI, and OCT measurements provide three-dimensional ocular biometry that can be used to construct personalized eye models, and ophthalmic measurements from Pentacam, Orbscan, or OCT scans provide both anterior and posterior corneal topography with microscopic accuracy. Another significant new measure is the wavefront aberration that can yield a detailed prescription of the eye's optical performance. These measurements can be incorporated into the creation of optically functional and analytical, personal-tailored, eye models.

Computational personalized eye models[7-9] are attractive since they preserve the necessary integrated ocular information to predict and describe selective ophthalmic phenomena. Sufficiency of the model is limited only by the relevant clinical data. Once constructed, they can be repeatedly used in contemporary optical design software to perform what resembles an in vivo quantitative evaluation of any ophthalmic optical system without the use of human subjects. Further, accurate simulations of clinical and diagnostic instruments will clearly be useful for

training medical professionals. This presentation will explore the feasibility of using personalized eye models for both normal and diseased eyes and will demonstrate examples.

We use two optical design programs, ZEMAX and the Advanced System Analysis Program (ASAP), to construct the 3-dimensional optical models. This base model is then modified to incorporate the clinically acquired patient data of ammetropic and keretoconus patients. The final models have identical clinical measured details and measurable optical performance.

Demonstrated in this paper are simulations of retinoscopy and infrared photorefraction. Using optical parameters of a common streak retinoscope and an infrared photorefraction device, the clinical observations and measurement of the diseased and normal retinal reflex patterns were simulated. To compare to the simulation results, the infrared photorefraction measurement were acquired from patients. Comparison of the retinal reflex images between the laboratory measurements and simulations were presented. These results show the viability of predictive medicine and possibly a revolutionary approach in developing optical instruments with eye modeling technique.

**Protocol Text:**

Figure 1 shows the diagram of eye modeling procedure. The step-by-step protocol is given below, and additional information is available in reference 10 [10].

***1.)*** **Create a generic eye model using contemporary optical software.**

**1.1.)** Use a lens design program such as the ZEMAX software package (www.optima-research.com), Code V (www.opticalres.com), or OSLO (www.lambdares.com) to construct a generic eye model that contains two corneal surfaces, one pupil stop, two lens surfaces, a retinal surface, and assign wavelength-dependent refractive indexes between surfaces. The Navarro 1985 model [2,3], Liou 1997 model [4], and Schwiegerling 1995 model [5] are well-accepted models that provide the necessary and anatomically accurate optical parameters. The step-by-step description for constructing Navarro and Liou models using ZEMAX can be found from the ZEMAX knowledge base website[11]. In this work, we use the Navarro model parameters for the base model and the ZEMAX program as the software for major eye model construction.

**1.2.)** Examine the eye's modulation transfer function (MTF) and point spread function (PSF) at the center of the field for the visible wavelength 550 nm. These eye models should have optical performance better than 20/20 (1 minute of arc resolution) for small pupils (2-4mm entrance pupil).

***2.)*** **Customize the model with patient's ocular biometry.**

**2.1.)** The first step is to substitute the cornea surface(s) of the base model with the patient's topography since it is the essential personalized ocular data.

2.1.1.) Make sure the topography data exported from the instrument is the elevation map, not power (dioptry) map. Examine the topography for missing data points due to occlusion from eye lash or eye lids. Repair and fill in the missing portion using an algorithm such as interpolation and extrapolation if necessary.

2.1.2.) Decompose the topography surface into Zernike polynomials series. $\Sigma\{Cnm\ Z(n,m)\}$. Make sure the Zernike radial order, n, is sufficiently large to preserve the detailed corneal information. Also, to prevent creating false information and introducing additional error,

the order, n, should be sufficiently low to ensure that the characteristic spatial frequency variations are smaller than the spatial frequency of data sampling.

2.1.3.) If both anterior and posterior corneal surfaces are measured (from Pentacam, Orbscan, or OCT), replace both surfaces from the base model with patient's topographies following step 2.1.2. Enter the cornea thickness along the optical axis, then, apply the coordinate break on the whole cornea (2 surfaces). Leave the coordinate shift and rotation at zero at this time. If only anterior topography is used, apply the coordinate break to only this surface.

**2.2.)** Substitute additional ocular parameters with the patient's ocular biometry data. These parameters may include the anterior chamber depth (ACD), lens thickness, vitreous chamber depth (VCD), and radii of curvatures of lens and retinal surfaces.

**2.3.)** Lens parameters are significantly dependent on the age. If ACD and lens parameters are not clinically available, replace them (from the base model) with age-dependent lens parameters from statistical investigation result [12].

***3.)*** **Incorporate patient's ocular aberration (optical performance) into the model**

**3.1.)** The ocular axial length (distance from cornea apex to retina) is significantly correlated to spherical equivalent refractive error. If the axial length was not obtained from the patient's eye, the first step is the optical optimization of axial length to approach the eye's spherical equivalent. If the wavefront aberration (WF) data are available, from these results the spherical equivalent can be calculated directly [13]. If WF was not obtained from the patient, use the manifest refractive error. When the axial length of the eye was available, this optimization can still be performed with an optimization tolerance corresponding to the standard deviation of the measurement. Note that this step may not be considered for modeling eyes with refractive errors that are resulting from abnormal mechanism such as keratoconus or cataract.

3.1.1.) Set the parameter of the vitreous chamber depth (VCD) as the iteration variable and assign tolerance for optical optimization.

3.1.2.) Set the light source at 550 nm wavelength and locate it at the eye's far-point position (reciprocal of the spherical equivalent). This can be done by applying a paraxial lens at cornea apex with a point source at infinity. The power of this paraxial lens should be equal to the best spherical correction (spherical equivalent) for the eye.

3.1.3.) Use ray aiming and perform optical optimization to obtain the sharpest focus on retina using default merit function. Select the RMS/spot size (SPD)/and reference to "Centroid" rather than "Chief Ray". Unless the optimization result is close to the diffractive limit, "RMS/ Wavefront/ Centroid" would not be considered. After optimization is performed, a new VCD value is obtained. Change the property of VCD from variable to constant.

**3.2.)** If wavefront aberration data are available, the second optimization is to approach this measured WF aberration, which is reported in Zernike polynomial format from most, if not all, of the current instruments.

3.2.1.) The optimization will be performed on crystalline lens parameters. In ZEMAX, change the lens surface type from standard surface to "Zernike standard sag", and the Zernike coefficients of this lens surface should be assigned as free variables for iteration. Assign all coefficients up to the same radial-order of the clinical wavefront data.

3.2.2.) In ZEMAX, the merit function will require the operand "ZERN". The optimization parameters may be set as Term=1, 2.. in the order of Zernike coefficients, Wave=1 (only one wavelength used in each of the calculations), Samp=2 (pupil sampling=64*64),

field=1 (only one field set in our calculations), and Type=1 (Zernike standard coefficient). Enter Zernike coefficients of the clinical WF data at the column of the "target" values.

3.2.3.) To allow for possible misalignment between the clinical WF and topography measurements, assign the coordinate break parameters of cornea as variables and allow small amounts of tolerances within the instrument's precision ranges.

3.2.4.) Assign the light source for the wavelength that was used in the clinical wavefront instrument. For example, WaveScan is 785 nm, LADAR is 820 nm, and Maxwell is 780 nm.

3.2.5.) For an optimization to typical 6-th or 7-th radial order of Zernike coefficients, an optimization can take from several minutes to many hours to complete if a single processor PC is used. Optimization is especially time consuming when the topography and the wavefront are very different in nature. The initial values for iteration are crucial for the minimizing computation time. The optimization can be performed using multiple optimization steps starting from the second order (3 variables) with coordinate break. Add variables one higher order at a time. By the end of optimization, the eye model should have identical wavefront aberration as measured data several digits down the wavelength.

**3.3.)** If wavefront aberration data are not available, use only the low-order aberration (i.e. refractive error) as the target of optical iteration.

3.3.1.) Since the vitreous chamber depth is restricted by the measured result or has been optimized to the eye's spherical equivalent, the iteration variable(s) in this step will be assigned to lens parameters. At least three variables are required. Astigmatism can be achieved by assigning two variables of perpendicular radii of curvature of either the lens surface and one variable on the rotation angle of the principle meridian. On occasion, the refractive index of the lens can be assigned as a variable of iteration.

3.3.2.) To produce the best sphero-cylindrical correction, assign the visible light point- source (550 nm) at infinity and at the cornea front apply two cylindrical paraxial lenses that are perpendicular to each other. Perform optimization for best retina focus using default merit function.

3.3.3.) After optimization, remove all paraxial lenses and change all iteration variables on lens surface to fixed constants. This is a "forward eye model".

**3.4.)** Export and use the final eye model parameters to construct a sequential backward model (from retinal surface to space of optical instrument) and a non-sequential model in program such as ASAP or ZEMAX.

***4.)*** **Validate eye model by patient vision simulation**

**4.1.)** Use the forward model to examine PSF and MTF performance of the eye at 550 nm wavelength.

**4.2.)** Perform letter-chart patient vision simulation.

4.2.1.) If available, for the pupil diameter use the eye's photopic pupil diameter. Otherwise, set the pupil size (optical entrance pupil) to 3mm.

4.2.2.) Use the image analysis option in the optical software to select the object image (letter E) and to assign the image dimension to correspond to 20/20 (5 minute arc). Locate the source image at 6 meter, and perform analysis to obtain the retinal image.

4.2.3.) Repeat 4.2.2 but change the image size to correspond to 20/30, 20/40, etc. resolution and obtain the retinal images.

4.2.4.) Compare the resulting retinal image with the uncorrected visual acuity (VA) record.

4.2.5.) Apply the ideal paraxial lens to remove the second-order aberration and then perform 4-2-1 to 4.2.4 to obtain letter-chart vision of the best-corrected VA (BCVA).

**4.3.)** Day and night vision can be simulated using the street scene input. Change the pupil size to 6mm or use the eye's scotopic pupil size for night vision simulation.

***5.)*** **Ophthalmic simulation:** Eye models can be imported and combined with optical system design in the software, ZEMAX or ASAP. Retinoscopy and infrared photorefraction simulation involve the double-pass procedures. The optical parameters and layout and the procedure of the retinoscopy simulation can be found in our previous work in open journal reference 9 [9]. The simulation of infrared photorefraction are described in our previous work in an open journal[8].

**5.1.)** The simulation can be performed with sequential ray tracing with a forward model to produce the retinal image and then use the result retinal image as the illumination source in a backward model to perform the return path simulation.

**5.2.)** An alternative approach is to use the non-sequential ray tracing ASAP program. Non-sequential ray tracing produces more realistic environment including options of surface and media scattering simulation. Without the restrictions of sequential ray tracing, the ray tracing is also more suitable for modeling diseased eyes that are far from ideal symmetric optics.

**Representative Results:** The simulated vision results represent the optical performance of the eye without taking into account the neural contribution. The visual performance simulation should achieve the quality of patient's vision or better. If the simulated results cannot reach the real eye's performance, the modeling procedure should be modified. The iteration variables and tolerances in the optimization steps must be selected carefully according to the pathology to mimic accurately the real eye. Two examples of the vision simulation results are shown in Figure 2. On the left are the incident letter images and the right are the retinal images of an astigmatic eye and a keratoconus eye. These results can be compared to patients' clinical record to validate the personal models.

Figure 3 shows the retinoscopy simulation result of a keratoconus eye as the projection of a streak retinoscope moves across the eye's astigmatic meridian. The scissors reflex is predicted. This type of simulation can provide an useful tool for medical training.

Figures 4 and 5 are the side-by-side comparison of simulation results of infrared photorefraction images with the experiment measurements of a myopic eye of the first author (Figure 4) and a keratoconus eye (Figure 5). The simulation results predict the structures of the retinal reflex measurements. The corneal reflections at the center of pupils are neglected in the simulation.

**Figures:** Please make sure that text in all tables or figures is made in **Arial** font. Figures should be submitted separately as layered .**tiff** or .psd files at **300 dpi**. All tables and figures should be given an appropriate title and should have a corresponding figure legend.

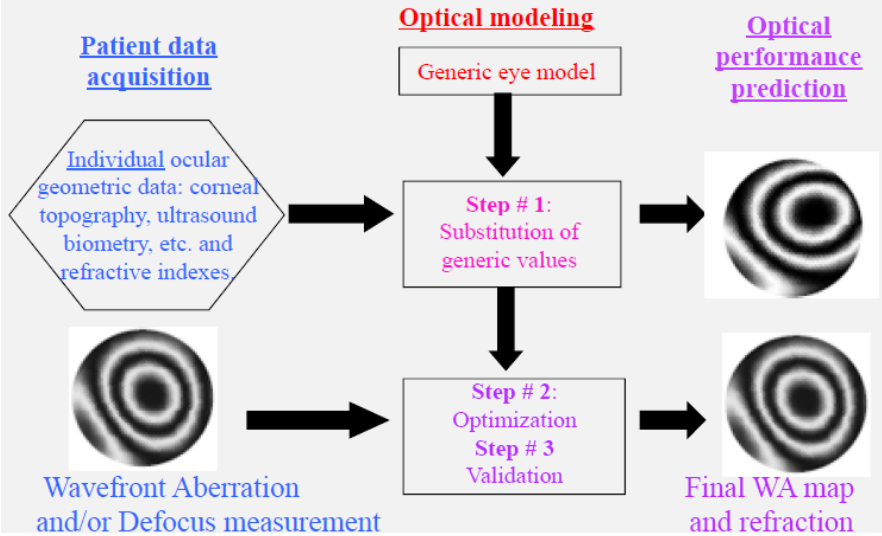


Figure 1. Diagram of personalized eye modeling procedure

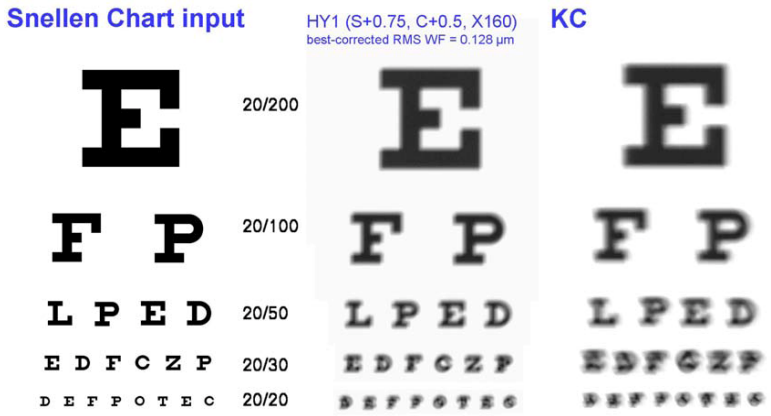


Fig. 2. Input letters (left) and the best-corrected Snellen chart vision of an astigmatic eye (middle) and a keratoconus eye (right)

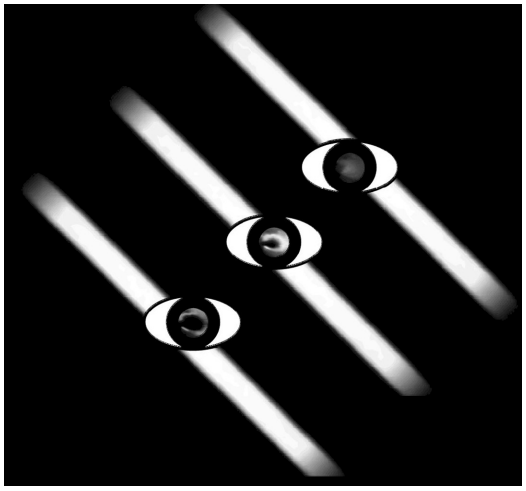

Figure 3. Retinoscopic simulation using a keratoconus eye.

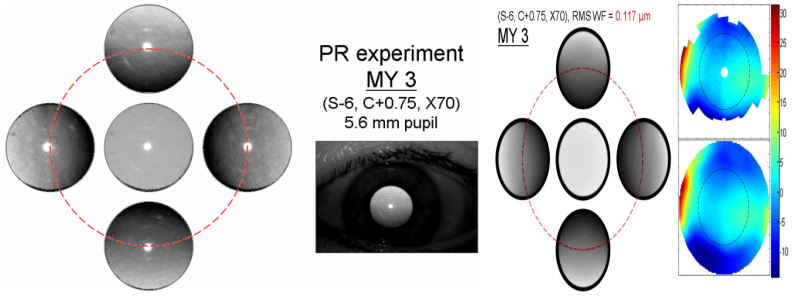


Fig. 4 (Left) 5 measured infrared PR myopic pupil reflex images (pupil only). (Middle) The lower one of the 5 original, unprocessed digital photograph. (Right) Simulated images using the personalized model of the patient.

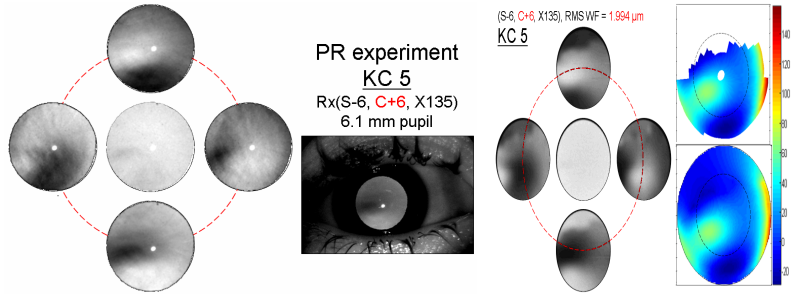


Fig. 5 (Left) 5 measured infrared PR keratoconus pupil reflex images (pupil only). (Middle) The lower one of the 5 original, unprocessed digital photograph. (Right) Simulated images using the personalized model of the patient.

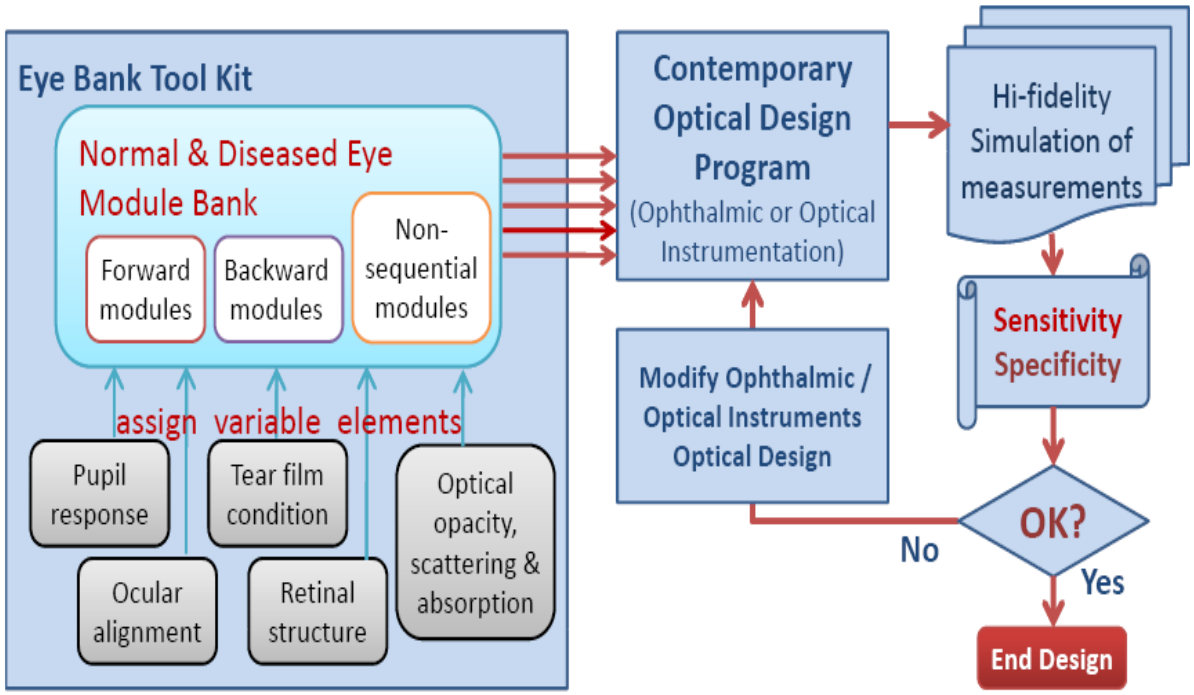


Figure 6 Diagram of Virtual Clinical Trial.

**Discussion:**

In this paper, we provide the customized modeling procedure and demonstrated eye modeling applications in medical training, patient consultation/education, and predicting instrument measurement.

Once a tool-kit of digital eye models of a particular population is established, the models can be used repeatedly in future applications. Development of modeling the retinal structure, tear film properties, optical opacities, ocular scattering, and a variety of ocular conditions will continue to expand the capacity of the eye model bank. As shown in Figure 6, the eyes' orientation, dilated or accommodative condition can be assigned, time-dependent tear film quality and cataract or floater conditions can also be introduced to simulate the sampling and environmental condition of a clinical trail. This capability provides a possibility to perform the evaluation of a new instrument's performance on computer with the desired eye population without intrusion to real human eyes. This is what we call the Virtual clinical trial.

This study shows the viability of predictive medicine and possibly a revolutionary approach in developing ophthalmic optical instruments with modeling technique.

**Acknowledgments:**

This project is supported by grant # 1R21EY018935-01A1 & R21 EY018385 from the National Eye Institute.

**Disclosures:**

The eye model bank for virtual clinical trial, medical training, and research applications is a novel idea and US patent # 7,607,776 B1 invented by the second and forth authors in this article.

**References:**


1. Gullstrand, A. The optical system of the eye, in *Physiological Optics*, 3rd ed. Vols 1 and 2, H. von Helmholtz (Hamburg, Voss, 1909), pp. 350-358.

2. Navarro, R., Santamaria, J., & Bescos, J., Accommodation-dependent model of the human eye with aspherics, J. Opt. Soc. Am. (A) 2, 1273-8 (1985).

1. Escudero-Sanz, I., & Navarro, R. Off-axis aberrations of a wide-angle schematic eye model. Journal of the Optical Society of America A, Optics, Image Science, and Vision, 16, 1881–1891. (1999).

2. Greivenkamp, J. E., Schwiegerling, J. Miller, J. M., & Mellinger, M. D. Visual acuity modeling using optical ray tracing of schematic eyes Am. J. Ophthalmol. 120, 227 (1995).

3. Liou, H. & Brennan N., Anatomically accurate, finite model eye for optical modeling, J. Opt. Soc. Am. A, 14, 1684-95 (1997).

4. Smith, G., & Atchison, D. A. The eye and visual optical instruments. Cambridge: Cambridge University Press. (1997).

5. Navarro, R., Gonzalez, L., & Hernandez-Matamoros, J. L. On the prediction of optical aberrations by personalized eye models. Optometry and Vision Science, 83, 371–381. (2006).

6. Chen, Y. L., Tan, B., Baker, K., Lewis, J. W., Swartz, T., & Wang, M. Simulation of keratoconus observation in photorefraction. Optics Express, 14, 11477–11485. (2006).

7. Tan, B., Chen, Y. L., Baker, K., Lewis, J. W. L., Swartz, T., & Wang M. Simulation of realistic retinoscopic measurement. Optics Express, 15, 2753–2761. (2007).

8. Chen, Y.L., Tan, B., Shi, L., Lewis, J. W. & Wang, M., Book chapter, Optical Eye Modeling and Applications, Computational Analysis of the Human Eye with Applications, editors: Sumeet Dua, Rajendra Acharya U, and E. Y. K. Ng, World Scientific Press (in press)

9. ZEMAX knowledge base website: http://www.zemax.com/kb/articles/186/1/How-to-Model-the-Human-Eye-in-ZEMAX/Page1.html, http://www.zemax.com/kb/articles/193/1/ZEMAX-Models-of-the-Human-Eye/Page1.html

10. Chen, Y.L., Tan, B., Shi, L., Lewis, J. W., Wang, M. & Baker, K, The shape of aging lens, *Invest Ophthalmol Vis Sci* 51: E-Abstract 4593. (2010)

11. Dorsch, R. G., Haimerl, W. A., & Esser, G. K. Accurate computation of mean power and astigmatism by means of Zernike polynominals. Journal of the Optical Society of America A, *15,* 1686-1688. (1998).